PRAMANA
— journal of
physics



Vol. 40, No. 4,
April 1993
pp. 299–309

# Prompt neutron emission spectra and multiplicities in the thermal neutron induced fission of $^{235}U$

M S SAMANT, R P ANAND, R K CHOUDHURY, S S KAPOOR, K KUMAR, D M NADKARNI and A SAXENA
Nuclear Physics Division, Bhabha Atomic Research Centre, Bombay 400085, India

MS received 25 January 1993

**Abstract.** The emission spectra of prompt fission neutrons from mass and kinetic energy selected fission fragments have been measured in $^{235}U(n_{th},f)$. Neutron energies were determined from the measurement of the neutron time of flight using a NE213 scintillation detector. The fragment energies were measured by a pair of surface barrier detectors in one set of measurements and by a back-to-back gridded ionization chamber in the second set of measurements. The data were analysed event by event to deduce neutron energy in the rest frame of the emitting fragment for the determination of neutron emission spectra and multiplicities as a function of the fragment mass and total kinetic energy. The results are compared with statistical model calculations using shell and excitation energy dependent level density formulations to deduce the level density parameters of the neutron rich fragment nuclei over a large range of fragment masses.

**Keywords.** Nuclear fission $^{235}U(n,f)$; neutron emission spectra; nuclear mass; total kinetic energy; neutron multiplicities.

**PACS No. 25·85**

## 1. Introduction

It is known that the prompt neutrons emitted in fission mostly result from the deexcitation of the excited fragment nuclei after they have acquired their full velocities. The emission spectra of the prompt neutrons in the rest frame of the emitting fragments can provide valuable information about the statistical properties such as temperature and level density of the neutron rich fragment nuclei. Detailed measurements of the neutron energy and its angle with respect to fragment direction as a function of fragment mass and kinetic energy are required in order to deduce, through kinematical transformation, the emission spectra in the rest frame of individual fragments, for carrying out direct comparison with the predictions of statistical cascade calculations. Although a number of measurements have been carried out in the past on neutron emission characteristics in low energy fission of various fissioning nuclei, there have been only a few detailed studies of the neutron emission spectra from individual fragments [1–7]. In the recent works [6, 7], the neutron emission spectra were analysed to deduce the effective temperatures and level density parameters for specified fission fragment masses in the case of spontaneous fission of $^{252}Cf$. The effective level density parameter was seen to have strong variations with fission fragment mass in the region of 120 to 150 amu. Similar detailed studies do not exist for other fissioning systems. In the present work, we report measurements on the neutron energy and multiplicities

in thermal neutron induced fission of $^{235}U$, as a function of fission fragment mass and kinetic energies. Detailed analysis of the data was carried out on the basis of the statistical model to deduce the neutron multiplicities, temperatures and level densities of the emitting fission fragments. The details of the experimental set up, data analysis procedure and results are discussed in the following.

## 2. Experimental set up

The experiments were performed using the thermal neutron beam from the CIRUS reactor at the Bhabha Atomic Research Centre in Bombay. Figures 1(a) and (b) show the time of flight set up used to measure the neutron energy spectrum along the direction of motion of the fragments. The energies of the two coincident fission fragments were recorded to enable the determination of fragment masses for each event. In the first set of measurements (figure 1(a)), the fission fragments were detected with a pair of surface barrier detectors, placed on either side of the $^{235}U$ target (100 $\mu g/cm^2$ electrodeposited on 160 $\mu g/cm^2$ Ni backing). The surface barrier detectors were located at 2·5 cm and 3·5 cm on either side of the target, which ensured that both the fragments were detected in coincidence without any bias due to loss of collinearity of the two fragments from the extended source and due to neutron emission effects. A 5 cm × 5 cm NE213 scintillation neutron detector was placed collinear to the two fragment detectors at a distance of 66·8 cm from the $^{235}U$ target. In this geometry, the neutrons making an angle of $\pm 10°$ to the direction of motion of the fission fragments were detected. The neutron detector was well shielded with

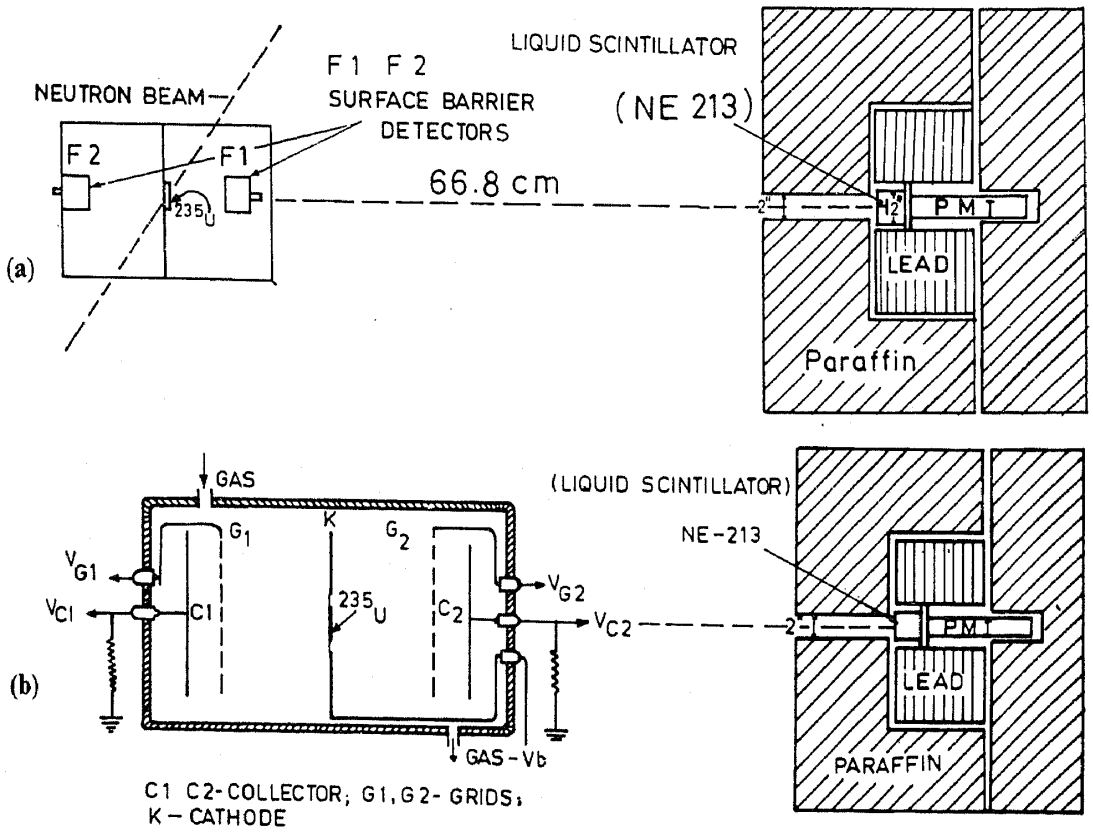


**Figure 1.** Schematic diagram of the TOF set-up: (a) The experiment with surface barrier detectors, (b) The experiment with ionization chamber.

7 cm of lead surrounded by 50 cm of borated paraffin in a cylindrical geometry in order to reduce the background. The pulse shape discrimination property of the NE213 detector was utilized to separate neutron and gamma events using the timing cross-over technique. The energy signals from the two fission detectors, the pulse shape and the energy signals of the neutron detector and the neutron time of flight, were recorded in list mode for further offline analysis.

In the second set of experiments, a back-to-back gridded ionization chamber was used to measure the energy and angle of both the fission fragments. As shown in figure 1(b), the chamber consisted of a central cathode and two parallel plate ionization chambers with frisch grids in a back-to-back geometry. The distance between the anode and the grid was 0·7 cm and between the cathode and grid it was 3·0 cm. A $^{235}U$ target of 100 $\mu g/cm^2$ thickness deposited on a thin gold coated VYNS backing was directly mounted in the centre of the cathode. The complete assembly was housed in a brass chamber, which was filled with P-10 gas at 1·1 atmosphere pressure. The gas was continuously purified by passing it over heated calcium filings. The neutron detector was placed at a distance of 70 cm from the uranium target along the electric field direction of the ion-chamber. The neutron time of flight was derived with the start signal taken from the common cathode of the ion-chamber and the stop signal taken from the neutron detector. The pulse heights of the signals from the collectors ($V_{C1}, V_{C2}$), the grids ($V_{G1}, V_{G2}$), the pulse shape and energy signals of the neutron detector, and neutron time flight were recorded in list mode for further offline analysis.

The method of analysis for the energy and angle determination of fission fragments from the collector and grid pulse heights followed the general procedure reported in the earlier works [8,9] with further improvements to correct for fragment energy loss in the target and backing material. Since the $V_g/V_c$ ratio is an indicator of the fragment angle, the energy loss correction to the grid and collector pulse heights ($V_g$ and $V_c$) were obtained from the observed shifts in the $V_c$ distribution as a function of $V_g/V_c$ ratio. The grid pulse height was calibrated for the fission fragment angle by fixing the 0° and 90° positions in the energy loss corrected grid pulse height distribution for each window on fission fragment mass and energy. These 0° and 90° grid pulse height values were fitted using the mass and energy dependent function as given in Rao *et al* [9]. The fragment angle could then be obtained from $V_g$ and $V_c$ data event by event. A more detailed description of the analysis method for the energy and angle measurements incorporating target thickness effects has been described elsewhere [10]. For the present studies to determine neutron emission spectra, only those fission events in which the fragments made an angle of less than or equal to $\pm$ 18° with respect to the electric field direction were analysed to deduce the neutron emission spectra from individual fragments.

## 3. Data analysis and results

About $2 \times 10^5$ and $1{\cdot}5 \times 10^6$ coincident events were recorded in the semiconductor based and ionization chamber based experiments respectively. The fragment energy calibration in both the experiments and also the angle calibration in the second experiment with the gridded ionization chamber, were done from the online unbiased singles data (without coincidence with the fission neutrons) by selecting fission events corresponding to the random background in the time of flight spectrum. The energies of the two fission fragments were determined after correcting for the target energy loss, pulse height defect of the silicon surface barrier detectors [11] and neutron

emission from fragments using data of Maslin *et al* [12]. The preneutron fragment masses and kinetic energies were obtained in an iterative way with the usual procedure based on the mass and momentum conservation relations. The preneutron emission average total kinetic energy of the fragments thus obtained was found to be 171·8 ± 1·5 MeV, in good agreement with other recent measurements [13, 14]. The resolution in the fragment mass determination was estimated to be about 2 to 3 mass units in both the experiments.

For measurements with the ionization chamber the data without coincidence with fission neutrons were analysed to obtain the calibration of the grid pulses for event by event angle determination. The method of analysis for angle determination using the grid and collector pulse heights has been described earlier in brief and the details of these have been given elsewhere [9, 10]. The angular resolution as determined from the difference between the angles of the complementary fission fragments measured on the two sides of the ionization chamber was seen to be 3° to 5° FWHM. The data corresponding to those events in which fragments were emitted in a cone of half angle of ± 18° with respect to electric field direction (direction of neutron detector) were analysed to determine neutron emission spectrum.

Figure 2(a) shows the neutron time of flight spectrum measured in the experiments. For the semiconductor detector experiment, the data were corrected for the spread in the time of arrival of the fission fragments in the semiconductor detector. The time resolution in both the experiments as determined from the FWHM of the prompt gamma peak was about 2 ns. The threshold of the neutron detector was set at 60 keV electron equivalent energy by using an $^{241}$Am source which is equivalent to a neutron energy of about 200 keV. The pulse shape discrimination spectrum is plotted in figure 2(b), which shows good separation between neutrons and gamma rays. The neutron events were selected offline by using a 2-dimensional gate on the time of flight and pulse shape signals of the neutron detector pulses. The detection efficiency of the neutron detector as a function of neutron energy was experimentally determined by measuring the neutron energy spectrum in $^{252}$Cf and $^{236}$U fission integrated over all angles and comparing with theoretical spectrum shapes. In the case of $^{252}$Cf fission, the source was mounted inside a mini-ionization chamber to detect the fragments in $2\pi$ geometry and the time of flight neutron spectrum was measured by placing the source in the same geometry as in the actual experiment. The measured $^{252}$Cf neutron spectrum was compared with the theoretical form of the energy spectrum given by Madland and Nix [15] to deduce the efficiency of the neutron detector. The efficiency of the neutron detector was also determined by comparing the measured neutron spectrum in $^{236}$U fission in $2\pi$ geometry with the known theoretical spectrum shape [16]. The efficiency values obtained by these two measurements were in agreement with each other as well as with the results of Monte Carlo calculations for the efficiency of the neutron detector, and were used in the analysis.

The multiparameter data of fragment kinetic energies and neutron time of flight (TOF) (and also of fragment-neutron angle in the ionization chamber based experiments) were analysed event by event. The laboratory neutron energy determined from the TOF data, was transformed to the centre of mass energy ($\eta$) after making the kinematic transformation involving the energy per nucleon of the emitting fragment. When the angle between the direction of motion of the neutron and the fragment is small as in the present case, due to strong focusing of the neutrons by the fragment motion, the neutrons detected in the neutron detector correspond predominantly to emission from the fragment moving towards the neutron detector.

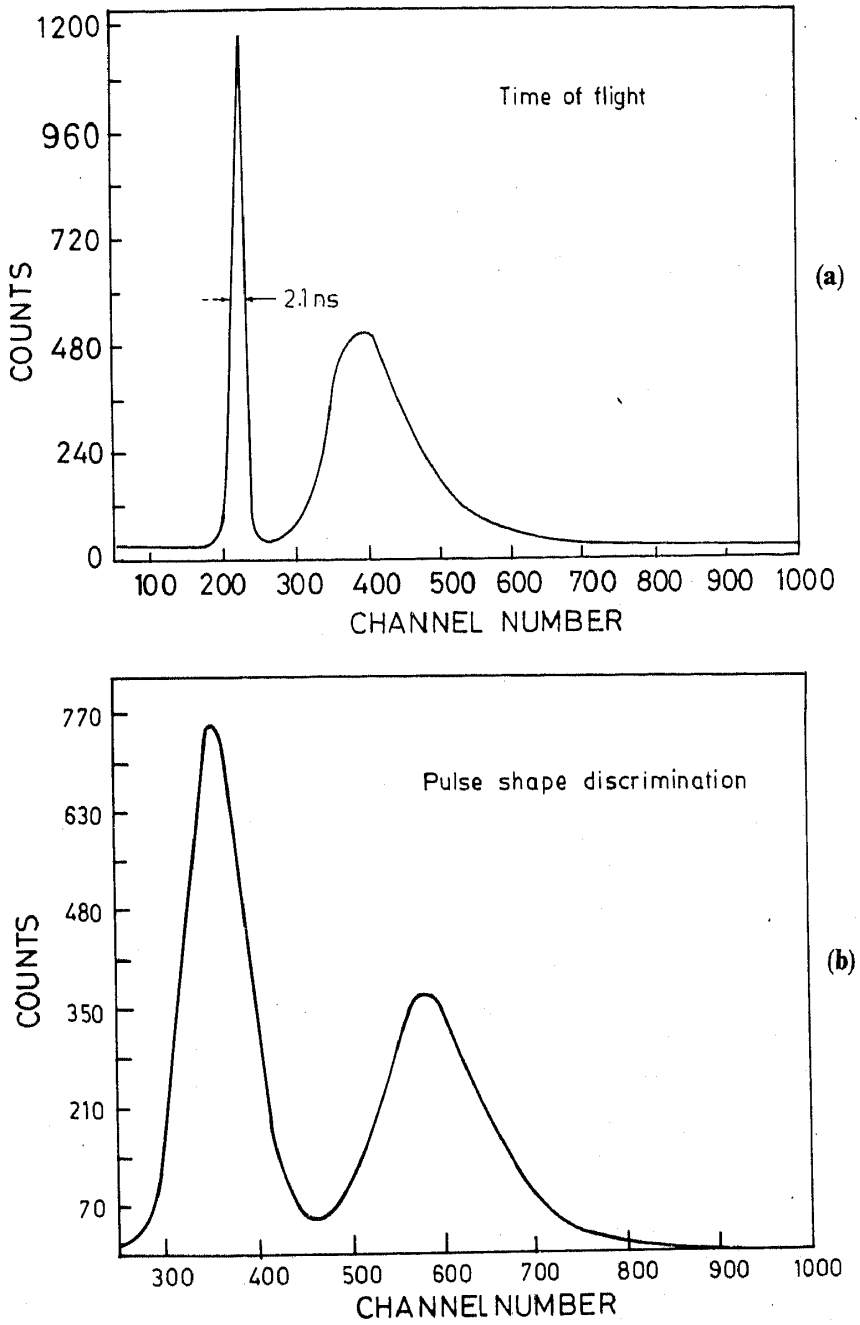


**Figure 2.** (a) Neutron time of flight spectrum in experiment-I, (b) Pulse shape discrimination spectrum in experiment-I.

Moreover, a very small fraction (less than a few per cent) of the neutrons emitted from the complimentary fragment moving in the opposite direction, which may appear in the forward direction, will have a very low energy close to the neutron detector threshold; thus it is justified to analyse the observed neutron spectra on the assumption that these neutrons are emitted by the fragment moving towards the neutron detector. Following the above procedure and after incorporating corrections for fragment recoil during neutron emissions, the centre of mass spectra were generated as a function of various mass groups in bins of two mass units. The background neutron contribution to the measured spectra were estimated from the average background per channel both on the left of the gamma peak and on the extreme right of the neutron tail

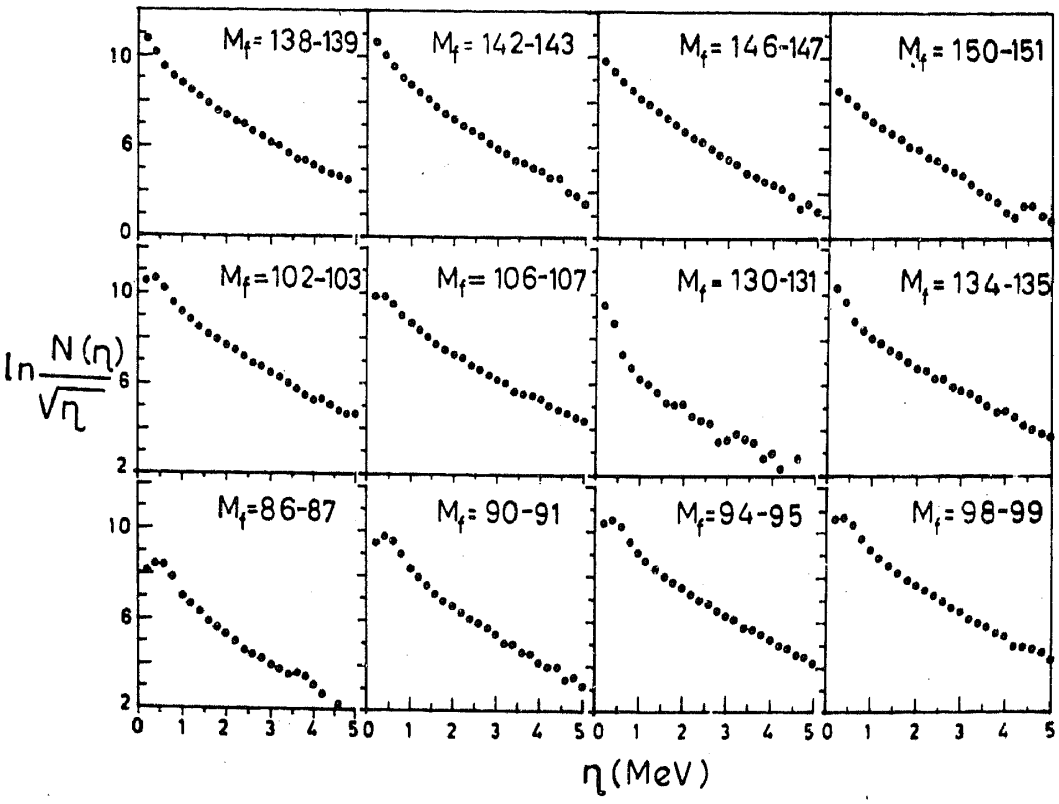


**Figure 3.** Plots of neutron centre-of-mass spectra for various fragment mass groups.

(below the neutron detector threshold) in the time of flight spectrum. The centre of mass neutron energy spectra obtained after background correction are shown in figure 3 in the form of plots of $\ln(N(\eta)/\sqrt{\eta})$ versus $\eta$ for several cases of selected fragment masses.

The neutron multiplicity was determined as a function of fission fragment mass and total kinetic energy for a mass bin of 2 amu and kinetic energy bin of 5 MeV. It was seen that the neutron multiplicity as a function of fission fragment mass reproduces the well known saw tooth curve in close agreement with earlier literature data. Figure 4 shows the neutron multiplicity ($\bar{\nu}$) as a function of the total kinetic energy ($E_K$) for typical fragment masses, where it is seen that the neutron multiplicity decreases as the $E_K$ increases implying the decrease in excitation energy of the fragments.

### 3.1 *Neutron energy spectra*

The centre of mass neutron energy spectra (neutron emission spectra) were analysed in the following manner. It was shown by Lecouteur and Lang [17], that the neutron emission spectrum can be represented as

$$N(\eta) = \text{Constant} * (\eta^{\lambda}/T_{\text{eff}}^{\lambda+1}) * \exp(-\eta/T_{\text{eff}}) \qquad (1)$$

where $T_{\text{eff}} = (11/12)\, T$ and $\lambda = 5/11$ for multiple neutron emission and $\lambda = 1$ for single neutron emission. It was also shown [17] that the energy spectrum gets further modified if evaporation takes place from a nucleus having a spread in the initial excitation energy.

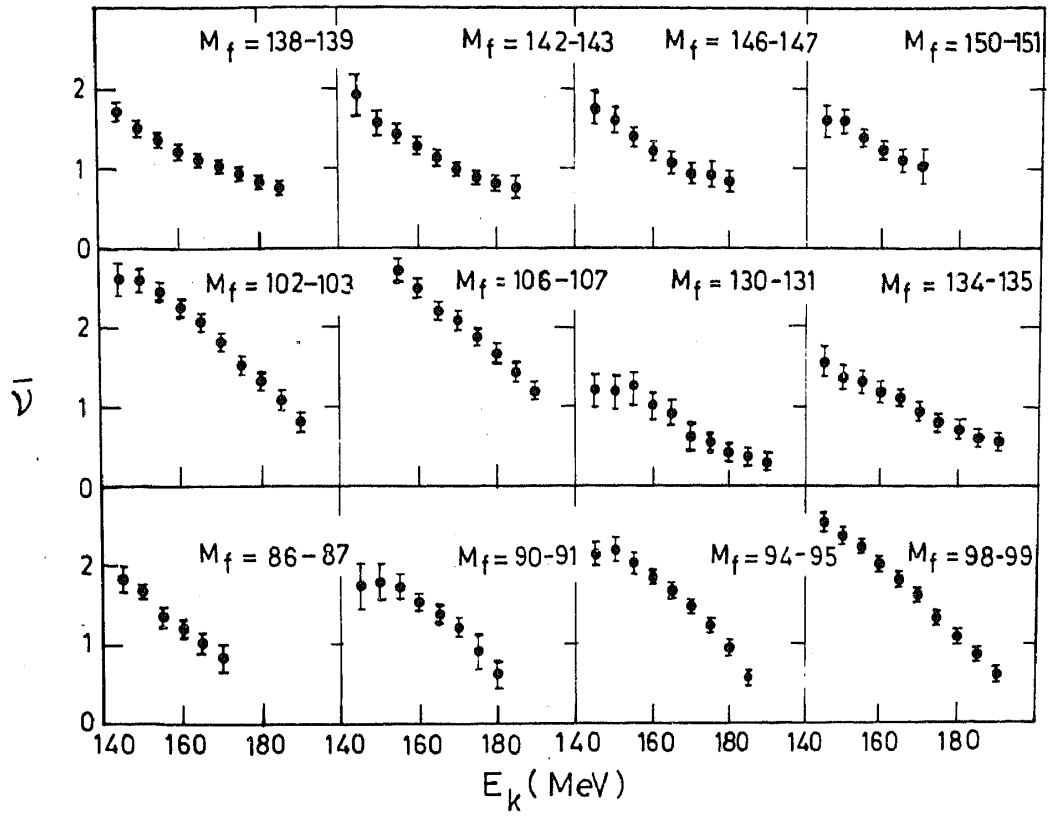


**Figure 4.** $\bar{\nu}$ vs. $E_K$ for various fragment masses.

In order to verify the parametric behavior of the energy spectrum we have carried out a systematic evaluation of the calculated neutron spectra using the evaporation code ALICE II [18] for various nuclei over a range of initial excitation energies taking into account the cascade emission effects. This evaporation code uses the standard Weisskopf–Ewing evaporation calculation with multiple particle emission where the particle emission probability is calculated using the standard optical model inverse reaction cross-sections and using spin and excitation energy dependent level density formulations. Neutron energy spectra were generated for various mass groups over a large excitation energy range (up to 30 MeV), using these calculations. The calculated spectra were then fitted to the expression,

$$N(\eta) = \text{Constant} * \eta^{\lambda} * \exp(-\eta/T_{\text{eff}}) \tag{2}$$

to determine the behavior of $T_{\text{eff}}$ and $\lambda$ with excitation energy for various fission fragment mass groups. It was seen that $T_{\text{eff}}$ and $\lambda$ follow the general trend suggested by the calculations of Lecouteur and Lang [17]. The measured neutron emission spectra from individual fragments were fitted to (2) to determine $T_{\text{eff}}$ assuming $\lambda = 1$ for cases when $\nu \leqslant 1$ and $\lambda = 0{\cdot}5$ when $\nu > 1$. The values of $T_{\text{eff}}$ as a function of the emitting fragment mass (summed over all kinetic energies), as deduced for the two sets of measurements, are shown in figure 5 and are found to be in agreement with each other.

### 3.2 *Determination of the level density parameter*

The results on the variation of $\bar{\nu}$ and $T_{\text{eff}}$ as a function of mass (figures 4 and 5) were used to determine the fragment excitation energy for carrying out statistical

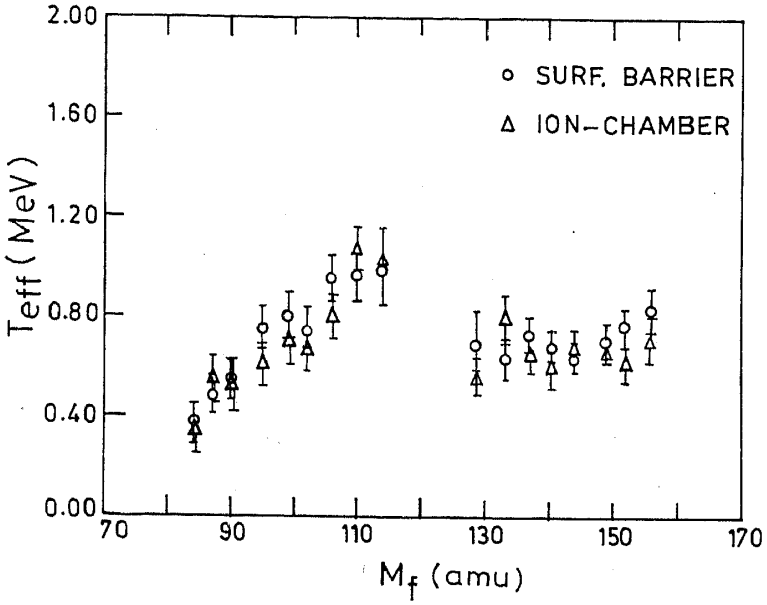


**Figure 5.** Variation of $T_{eff}$ with fragment mass. (o o o – Experiment-I, Δ Δ Δ – Experiment-II).

evaporation calculations to obtain information on the level density parameter as a function of fragment mass.

The average excitation energy of fragments of specified mass and $E_K$ was calculated by the following relation

$$E_X(M_f, E_K) = \bar{\nu}(M_f, E_K) * [B_n(M_f) + 3/2\, T(M_f, E_K)] + E_\gamma(M_f)$$

where $B_n(M_f)$ is the neutron binding energy for the particular mass group averaged over various fragment atomic numbers, and $E_\gamma$ $(M_f)$ is the average energy released by gamma emission. The $B_n(M_f)$ values were calculated after averaging over the fragment charge distributions, and using the values of the neutron binding energies from the mass tables (atomic mass adjustment tables [19]). The $E_\gamma(M_f)$ values were taken from the data of Pleasonton *et al* [20]. The total excitation energies of the fragments obtained by adding the excitation energies of the complementary fragments were found to be in agreement with the estimates obtained from total kinetic energy measurements [14] within about 2 MeV. The excitation energies calculated as above for individual fragment masses were used as inputs to calculate the neutron emission spectra using the evaporation model code ALICE II, which was modified so that the level density formulations could be changed as desired. The present calculations were done after incorporating a shell dependent level density formula [21]. This formula takes into account the excitation energy dependence of shell effects in such a way that, the level density parameter $a$ used in the formulations corresponds to the Fermi gas model and is independent of shell effects. The ground state shell correction energies which go as inputs for the level density calculations were taken from the experimental shell correction energies given by Seeger and Howard [22]. These values were also suitably averaged to take into account the fragment charge distributions and spread in the masses for each mass group. Evaporation cascade calculations were carried out with a distribution in the excitation energy of each fragment for which the average was taken as mentioned above and the variance $(\sigma^2_{Ex})$ was estimated from the observed spread in the total fragment kinetic energy distributions [14]. It was assumed that

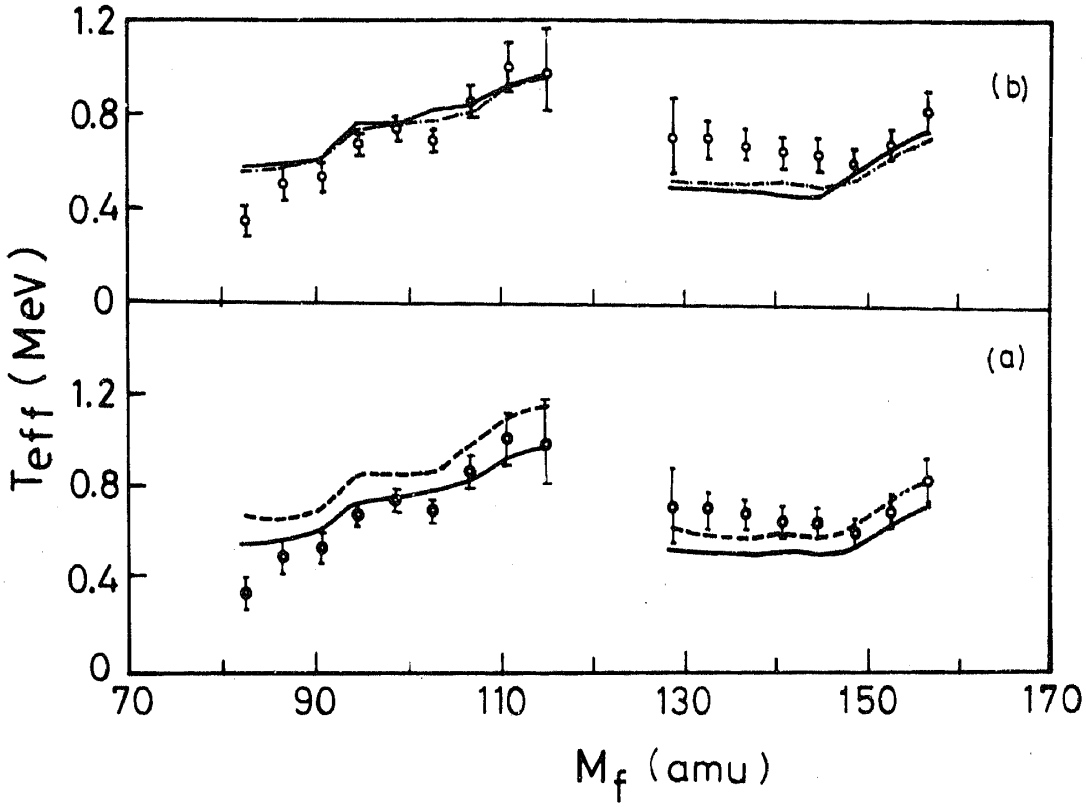


**Figure 6.** (**a**) Comparison of experimental and calculated values of $T_{eff}$ as a function of fragment mass. Calculations include shell corrections in the level density formula (○ ○ ○ ○ – experimental values; ——— – calculation with $a = A/7$; _____ calculation with $a = A/10$). (**b**) Comparison of experimental and calculated values of $T_{eff}$ with (–·–·–·–) and without (————) inclusion of shell correction in the level density formula for $a = A/7$.

the excitation energy spread of each fragment is in proportion to its average excitation energy [5]. The calculations were carried out by varying the level density parameter $a$ and also with and without the shell correction in the level density expression to estimate the relative importance of the various parameters in the determination of neutron energy spectra. The calculated neutron spectra were fitted to the form given by (2), as were the experimental spectra, and the $T_{eff}$ values obtained by these calculations are compared with the experimental values in figures 6(a) and 6(b). It is seen from figure 6 that the calculated $T_{eff}$ values are sensitive to the level density parameter $a$, but are only marginally affected by the inclusion of shell corrections in the level density formula. The calculated results are, therefore, not affected by any uncertainties in the shell correction energies. It was also found that in the mass region A = 128–134 amu where the average excitation energies are small there is a marked effect of the inclusion of spread in the excitation energy of the fragments on the calculated $T_{eff}$ values. It is seen from the figure that, in general, a better fit is obtained for all fragments with the level density parameter $a = A/7$, except in the mass region of A = 128–140 amu, where $a = A/10$ gives a closer agreement to the experimental data.

In an alternative way the level density parameter can also be derived from the detailed analysis of the $T_{eff}$ for specific mass and excitation energies [7]. The experimentally measured values of $T^2$ ($\approx 1{\cdot}2T_{eff}^2$) are plotted in figure 7 as a function

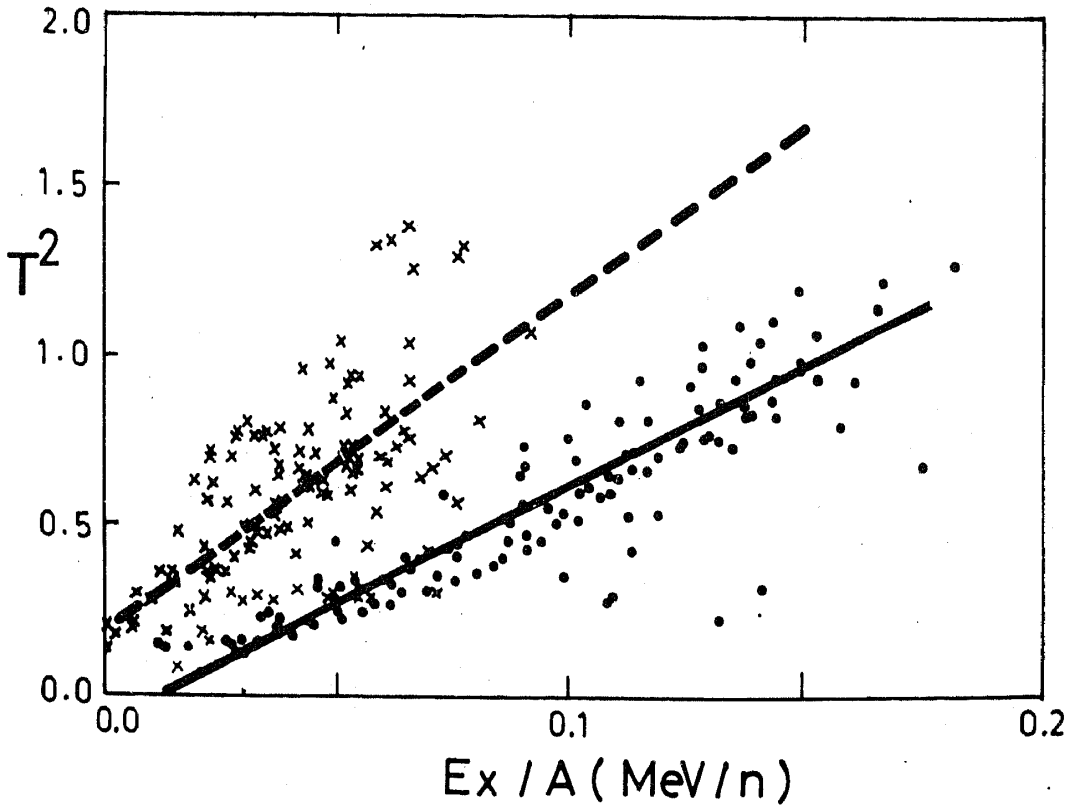


**Figure 7.** $E_X/A$ vs $T^2$ (——— $a = A/7$, ——— $a = A/10$, ● ● ● light fragments, × × × heavy fragments).

of the residual excitation energy per nucleon after one neutron emission for the light and heavy fragments. Two straight lines corresponding to the level density parameter $a = A/7$ and $a = A/10$ have also been drawn in these figures. There is a considerable scatter of the experimental points about these lines which is to be expected due to this simplified picture and also the spread in the excitation energy of the fission fragments about the average value. It is seen that the line corresponding to $a = A/7$ shows the average variation of the data points for the light fragments, whereas for the heavy fragments the line corresponding to $a = A/10$ follows the average variation of the data points more closely.

The present analysis therefore consistently shows that the mass dependence of the level density parameter $a$ is different in the light and the heavy fragment groups. The reason for such a different behavior of $a$ in different fragment mass regions is not very clear at present, and needs to be theoretically investigated further.

## 4. Conclusion

Neutron emission spectra from specified mass and kinetic energy selected fission fragments were determined in thermal neutron induced fission of $^{235}U$ using two independent experimental techniques for fragment energy measurements. The results were analysed to determine the neutron multiplicities and temperatures of excited neutron rich fragments. Comparison of the measured neutron emission spectra with the statistical model evaporation cascade calculations, after incorporating proper spread in the excitation energy of the fission fragments, show that it is difficult to fit the spectra for both the light and the heavy mass groups with a single level density

parameter, and level density parameter $a = A/7$ for the light fragments, and $a = A/10$ for the heavy fragments give best fit to the measured spectra.

**Acknowledgement**

One of us (MSS) would like to thank the Department of Atomic Energy and Board of Research in Nuclear Sciences, for providing him the fellowship to carry out this research work.

**References**

[1] H R Bowman, S G Thomson, J C D Milton and W J Swiatecki, *Phys. Rev.* **126**, 2120 (1962)
[2] S S Kapoor, R Ramanna and P N Ramarao, *Phys. Rev.* **131**, 283 (1963)
[3] J C D Milton and J S Fraser, *Proc. Symp. Phys. and Chem. of fission*, Salzburg, (1965) Vol. II p. 39
[4] K Skarsvag and K Bergheim, *Nucl. Phys.* **A163**, 82 (1970)
[5] H Nifenecker, C Signarbieux, R Babinet and J Poitou, *Proc. Symp. on Phys. and Chem. of fission*, Rochester, (1973) Vol. 2 p. 117
[6] E A Sergina and P P Dyachenko, *Yad. Fiz.* **42**, 1337 (1985)
[7] C Budtz-Jorgensen and H H Knitter, *Nucl. Phys.* **A490**, 307 (1988)
[8] R K Choudhury, S S Kapoor, D M Nadkarni and P N Ramarao, *Nucl. Instrum. Methods* **164**, 323 (1979)
[9] M N Rao, S R S Murthy and R K Choudhury, *Nucl. Instrum. Methods* **A313**, 227 (1992)
[10] M S Samant, R P Anand, R K Choudhury, D M Nadkarni and S S Kapoor, *Proc. Int. Conf. Nucl. data for Sci. Tech.*, Julich, Germany, May 18–22 (1991)
[11] H W Schmitt, J H Neiler and F J Walter, *Phys. Rev.* **B137**, 837 (1965)
[12] E E Maslin, A L Rodgers and W G F Core, AWRE Report No. 0–43/67, (1967)
[13] C Budtz-Jorgensen, H H Knitter, Ch Straede, F-J Hambsch and R Vogt, *Nucl. Instrum Methods* **A258**, 209 (1987)
[14] M N Rao, 1990 *Mass energy and charge correlation studies of fragments in low energy fission*, Ph.D. Thesis, Utkal University, India
[15] D G Madland and J R Nix, *Proc. Int. Conf. Nucl. data for Sci. Tech.* Antwerp, Belgium, Sept. 6–10, (1982) p. 473
[16] J Neill, Report **GA-9753**, (1969)
[17] K J LeCouteur and D W Lang, *Nucl. Phys.* **13**, 32 (1959)
[18] M Blann, LLNL Report No. UCID-20169, (1984) (unpublished)
[19] Atomic Mass Adjustment Tables 1983 Nuclear Data Section IAEA
[20] F Pleasonton, R L Ferguson and H W Schmitt, *Phys. Rev.* **C6**, 1023 (1972)
[21] S K Kataria, V S Ramamurthy and S S Kapoor, *Phys. Rev.* **C18**, 549 (1978)
[22] P A Seeger and W M Howard, *Nucl. Phys.* **A238**, 491 (1975)